Enhancing the conductivity of transparent graphene films via doping

2010 Nanotechnology 21 285205

(http://iopscience.iop.org/0957-4484/21/28/285205)

Nanotechnology **21** (2010) 285205 (6pp) doi:10.1088/0957-4484/21/28/285205

Enhancing the conductivity of transparent graphene films via doping

Ki Kang Kim[1], Alfonso Reina[2], Yumeng Shi[3], Hyesung Park[4], Lain-Jong Li[3], Young Hee Lee[5,6] and Jing Kong[1,6]

[1] Department of Electrical Engineering and Computer Sciences, Massachusetts Institute of Technology, Cambridge, MA 02139, USA
[2] Department of Material Science, Massachusetts Institute of Technology, 77 Massachusetts Avenue, Cambridge, MA 02139, USA
[3] School of Materials Science and Engineering, Nanyang Technological University, 50 Nanyang Avenue, Singapore 639798, Singapore
[4] Department of Mechanical Engineering, Massachusetts Institute of Technology, Cambridge, MA 02139, USA
[5] BK21 Physics Division, Department of Energy Science, Center for Nanotubes and Nanostructured Composites, and Sungkyunkwan Advanced Institute of Nanotechnology, Sungkyunkwan University, Suwon 440-746, Korea

E-mail: leeyoung@skku.edu and jingkong@mit.edu

Received 21 January 2010, in final form 7 April 2010
Published 28 June 2010
Online at stacks.iop.org/Nano/21/285205

Abstract
We report chemical doping (p-type) to reduce the sheet resistance of graphene films for the application of high-performance transparent conducting films. The graphene film synthesized by chemical vapor deposition was transferred to silicon oxide and quartz substrates using poly(methyl methacrylate). $AuCl_3$ in nitromethane was used to dope the graphene films and the sheet resistance was reduced by up to 77% depending on the doping concentration. The p-type doping behavior was confirmed by characterizing the Raman G-band of the doped graphene film. Atomic force microscope and scanning electron microscope images reveal the deposition of Au particles on the film. The sizes of the Au particles are 10–100 nm. The effect of doping was also investigated by transferring the graphene films onto quartz and poly(ethylene terephthalate) substrates. The sheet resistance reached 150 Ω/sq at 87% transmittance, which is comparable to those of indium tin oxide conducting film. The doping effect was manifested only with 1–2 layer graphene but not with multi-layer graphene. This approach advances the numerous applications of graphene films as transparent conducting electrodes.

S Online supplementary data available from stacks.iop.org/Nano/21/285205/mmedia

(Some figures in this article are in colour only in the electronic version)

1. Introduction

Recently graphene has emerged as a fascinating 2D system in condensed-matter physics as well as a new material for the development of nanotechnology. The unusual electronic band structure of graphene allows it to exhibit a strong ambipolar electric field effect with high mobility [1]. Each graphene layer has a very low opacity of 2.3% [2]. These properties lead to the possibility of its application in high-performance transparent conducting films (TCFs) [3].

The exfoliated graphite or graphite oxide has been suggested as one of the candidate materials for TCFs [4–6]. However, their sheet resistances were still higher than those of carbon nanotube-based TCFs and indium tin oxide [7, 8]. Recently, large area graphene synthesized by vacuum graphitization using silicon carbide or a chemical vapor deposition (CVD) method using a Ni or Cu catalyst has been demonstrated by several groups [3, 9–18]. After the CVD synthesis, the graphene film can be transferred to a target substrate using poly(methyl methacrylate) (PMMA) or poly(dimethylsiloxine) (PDMS) [3, 11, 14, 17]. The

[6] Authors to whom any correspondence should be addressed.

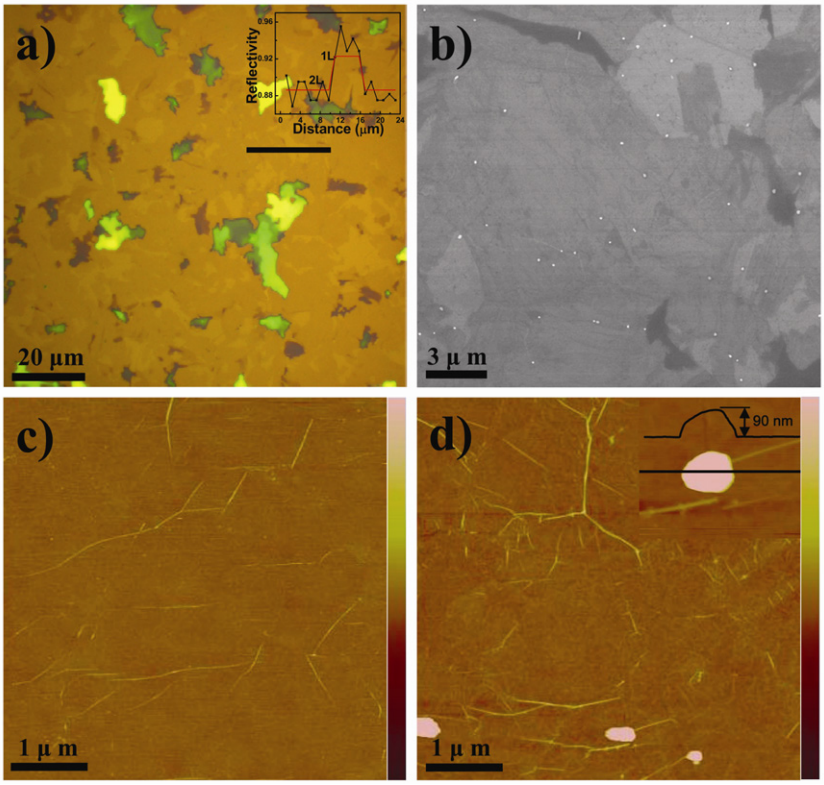

Figure 1. The morphology of a graphene film transferred onto 300 nm SiO_2/Si. (a) Optical image of graphene. The inset shows the different reflectivities at 532 nm (green) for monolayer and bilayer graphene. (b) SEM images after 5 mM $AuCl_3$ doping. The bright spots indicated the reduced Au particles. AFM images of (c) clean graphene and (d) after 5 mM doping. The inset in (d) shows that the gold particle was formed on the graphene wrinkle. The side scale bar height is 30 nm.

advantage of the CVD and transfer method is that the size of the graphene film can be easily scaled up, and the overall process can be relatively inexpensive. These approaches enable us to fabricate highly transparent conducting electrodes with the graphene films. Compared to indium tin oxide (ITO) electrodes, which have a typical sheet resistance of 5–60 Ω/sq and ∼85% transmittance in the visible range (400–900 nm) [8], the CVD-grown graphene electrodes have a higher/flatter transmittance in the visible to IR region and are more robust under bending [3]. Recently, Li *et al* have reported that four layers of graphene has the sheet resistance of 350 Ω/sq at about 90%; these were prepared on glass with the PMMA transfer method after growing graphene on Cu [19]. Nevertheless, the lowest sheet resistance of the currently available CVD graphene electrodes is higher than that of ITO.

In this paper, we report using $AuCl_3$ chemical doping as a way to improve the film conductivity of the CVD-grown graphene. By optimizing the doping concentration, the lowest sheet resistance of 150 Ω/sq at 87% transmittance was obtained, which was comparable to those of ITO films. The charge transfer by reduction of Au^{III} to Au particles was monitored by Raman spectroscopy. The reduction of the sheet resistance was manifested for single- and bi-layer regions of graphene and no significant doping effect was observed with multi-layer graphene layers.

2. Experimental details

2.1. Synthesis of graphene and transfer

Large area graphene film was synthesized by the CVD method as previously reported [11, 18]. A substrate with a 300 nm Ni film sputtered on SiO_2/Si at 450 °C was placed in the CVD chamber with a gas flow rate (H_2:Ar = 400:600 sccm) for 20 min at 1000 °C in order to smooth the Ni surface and to activate the Ni grain growth. CH_4 (4 sccm) along with H_2 (1400 sccm) was then flowed at 1000 °C for 5 min in order to carburize the Ni film. Finally, to control the graphene film thickness, the Ni film was cooled down to 500 °C with a cooling rate of 5 °C min^{-1} under CH_4:H_2:Ar = 4:700:700 sccm. One or two graphene layers were formed in most areas. The graphene film was transferred by the following method using PMMA: after deposition of PMMA (9% in anisole) on graphene film, the substrate was baked at 120 °C for 20 min. To detach the Ni and graphene film from SiO_2/Si substrate, the PMMA substrate was floated in 19% HCl for 5 min. To remove the residual Ni film, the PMMA film was placed in nickel etchant (TFB, Transene Company, INC) for 1 h followed by neutralization with deionized water for 1 h. The resultant film with PMMA and graphene was then transferred to a 300 nm SiO_2/Si substrate or quartz substrate. To remove the PMMA completely, the substrate was annealed under a gas flow rate (H_2:Ar = 700:400 sccm) for 90 min in the CVD chamber.

2.2. Doping with $AuCl_3$

$AuCl_3$ is a commonly used compound in doping organic conducting polymers such as poly(3-alkylthiophene) and poly(3-octylthiophene) [20, 21]. If graphene could be regarded as a π-conjugated polymer from the structural point of view, the doping mechanism should be similar. When $AuCl_3$ is dissolved in a solvent, depending on the amount of coordinating agent, a different ionic conformation could result. Water or acetonitrile preferentially lead to a square planar geometry of $AuCl_4^-$ [20]. In this study we mainly used nitromethane as a solvent, which is a poor coordinating solvent, and it is understood that the following reactions will take place [20]:

$$2\text{Graphene} + 2AuCl_3 \rightarrow 2\text{Graphene}^+ + AuCl_2^- (Au^I) + AuCl_4^- (Au^{III}) \quad (1)$$

$$3AuCl_2^- \leftrightarrow 2Au^0\downarrow + AuCl_4^- + 2Cl^-. \quad (2)$$

That is, there is the reduction of Au^{III} to Au^I [20], and uncoordinated Au^I disproportionately to form $AuCl_4^-$, Au^0, and Cl^-.

In the presence of excess $AuCl_3$, Cl^- coordinates according to

$$Cl^- + AuCl_3 \rightarrow AuCl_4^-. \quad (3)$$

Furthermore, if other solvents (e.g., water) are used, $AuCl_4^-$ can be directly reduced by [22]

$$AuCl_4^- + 3e \rightarrow Au^0\downarrow + 4Cl^-. \quad (4)$$

Graphene could be p-doped via reaction of (1)–(3) or (4) with different reduction potentials of 1.4 V and 1.0 V, respectively.

The graphene films were doped as a function of $AuCl_3$ concentration (Sigma Aldrich). 200 μl of mixed $AuCl_3$ in nitromethane (Sigma Aldrich) with different $AuCl_3$ concentration was dropped onto the graphene film and spun at 2500 rpm for 60 s.

2.3. Measurement

The sheet resistance of the sample was measured by the 4-probe van der Pauw method. Its surface morphology was observed by scanning electron microscopy (SEM) (6320V field-emission high-resolution SEM, JEOL) and atomic force microscopy (AFM) (Dimension 3100, Veeco). The transmittance of the sample was obtained by UV–vis–NIR measurement (Cary 5E, Varian). To confirm the charge transfer, the sample was analyzed by Raman spectroscopy with a laser excitation energy of 532 nm (2.33 eV).

3. Result and discussion

3.1. Surface morphology after doping

The number of layers for the graphene films transferred on 300 nm SiO_2/Si is distinguishable by the color contrast through the optical microscope [18, 23–25]. Figure 1(a) shows the optical image of CVD-grown graphene transferred onto 300 nm SiO_2/Si. There are some thicker graphene layers which grew between Ni grain boundaries. The inset in figure 1(a) indicated the different reflectivities at 532 nm

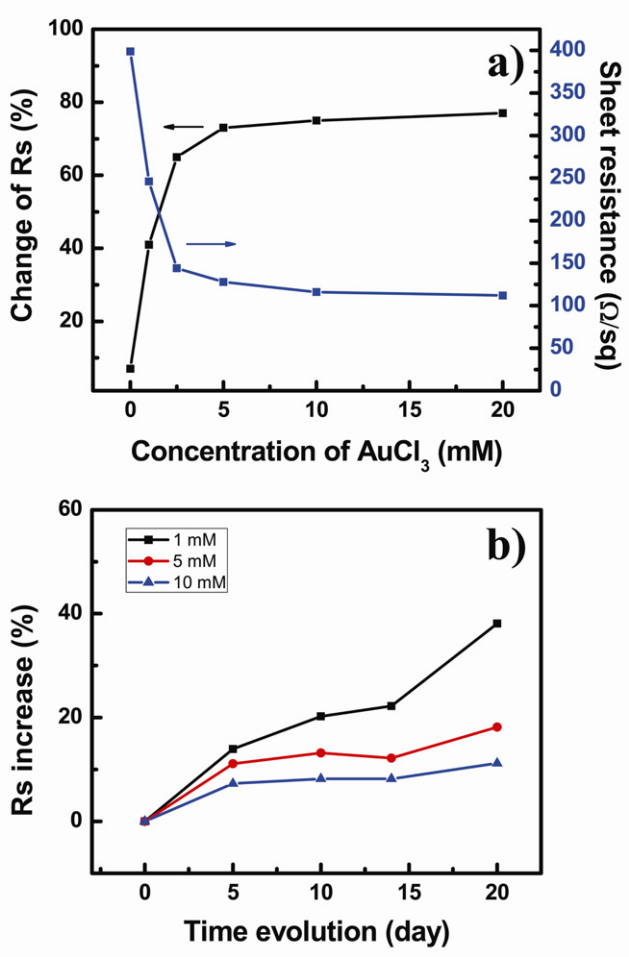

Figure 2. Sheet resistance measurement (R_s) (a) before and after $AuCl_3$ doping as a function of $AuCl_3$ concentration and (b) doping stability with time evolution at room temperature under ambient atmosphere.

(green color) for monolayer and bilayer graphene. This is a very useful method to distinguish the number of layers up to three layers [18]. The PMMA was completely removed, as shown in the AFM image in figure 1(c). The roughness of the transferred graphene film measured by the AFM was less than 0.3 nm. We found the neutralization process was very important to remove the PMMA with the annealing process. After doping with 5 mM $AuCl_3$, the Au particles in figure 1(b) were uniformly formed on the graphene film. Because the reduction potentials of Au^{III}, which are 1.4 and 1.0 V for reaction (1)–(3) and reaction (4), respectively, are higher than that of graphene, 0.22 V [26, 27][7], Au^{III} can be easily reduced on the graphene. The density of Au particles increased as the doping concentration increased (see the supporting information (SI) figure S1 available at stacks.iop.org/Nano/21/285205/mmedia). The gold particles formed on the graphene surface were further confirmed by energy dispersive x-ray analysis (EDX) (see the supplementary data, figure S2 available at

[7] The reduction potential of graphene can be calculated as $W/e = V$ (versus NHE)+4.44(V), where W is the work function of graphene and V is the reduction potential versus a normal hydrogen electrode (NHE) [26]. Since the work function of graphene is 4.66 eV, the reduction potential of graphene is 0.22 V [27].

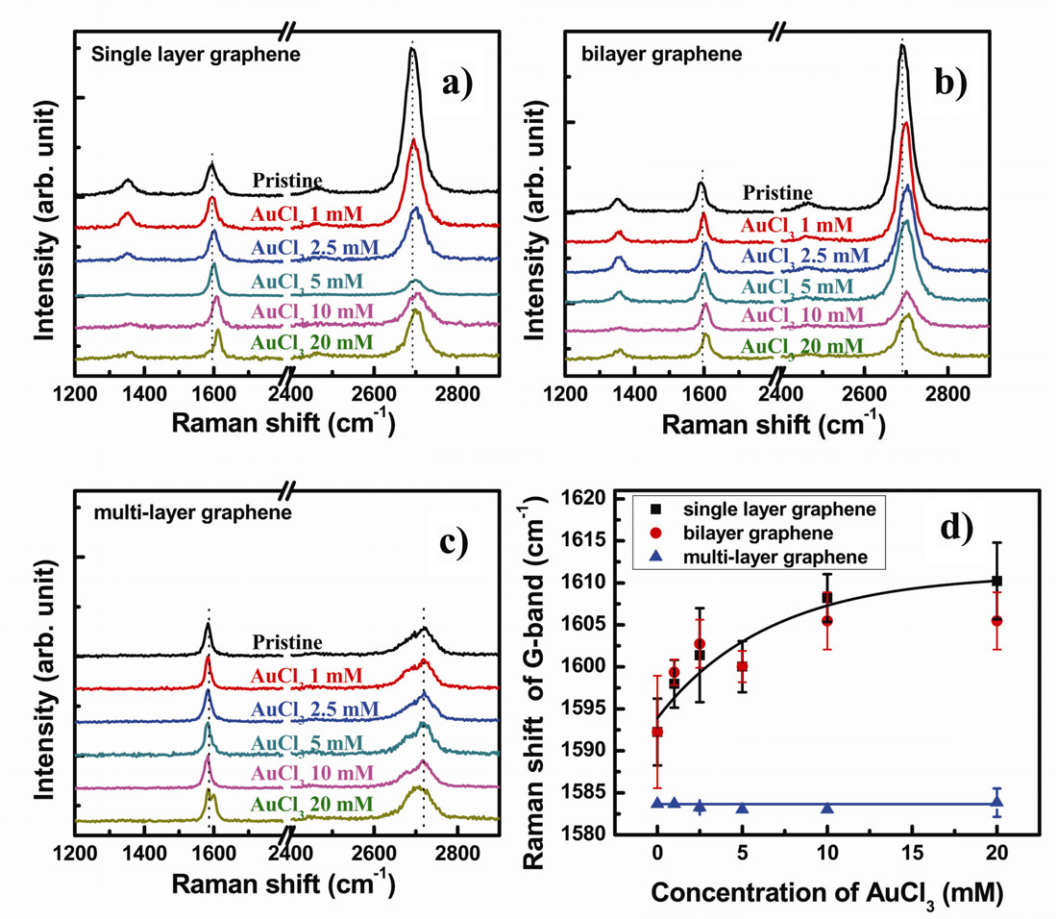

Figure 3. Raman spectra of (a) single-, (b) bi-, and (c) multi-layer graphene with a laser excitation energy of 523 nm (2.33 eV) as a function of $AuCl_3$ concentration. (d) G-band shift of single-, bi-, multi-layer graphene. The G-band was upshifted up to 12 cm^{-1} in the case of single- and bi-layer graphene. However, the G-band of multi-layer graphene was not changed.

stacks.iop.org/Nano/21/285205/mmedia). To elucidate the Au particle formation on the graphene surface, the graphene film was characterized by AFM. Figure 1(c) shows the AFM image of the graphene surface, with wrinkles which could come from the nucleation of defect lines on the step edges, thermal-stress-induced formation or the sample preparation procedure [16]. Au particles with sizes in the range 10–100 nm were formed on the graphene wrinkles, as shown in figure 1(d) (see the supplementary data, figure S3 available at stacks.iop.org/Nano/21/285205/mmedia). We found that most of the Au particles had sizes ranging between 10 and 100 nm, independent of the concentration of $AuCl_3$. Ideal graphene has de-localized π-electron states which have a direction perpendicular to the carbon atom surface. This makes it stable under ambient conditions [28]. It is still possible that the curvature induced by the wrinkles makes the wrinkles more reactive than the flat region. This is similar to the case of carbon nanotubes, that is, smaller diameter nanotubes are more reactive due to a curvature effect [29]. As a result, most of the Au particles were found on the graphene wrinkles.

3.2. The change of electrical property

To study the change of the sheet resistance (R_s) after doping, the R_s of the transferred few layers graphene film on 300 nm SiO_2/Si was measured by a 4-probe measurement. The R_s of the few layers graphene ranged between 450 and 550 Ω/sq. Figure 2 shows the percentage change of R_s (defined as $100 \times (\frac{R_{s\,\mathrm{before}} - R_{s\,\mathrm{after}}}{R_{s\,\mathrm{before}}})\%$) and the absolute R_s as a function of $AuCl_3$ concentration. As the concentration of $AuCl_3$ increased, the R_s first decreased dramatically. The change of R_s saturated to 77% with a 112 Ω/sq sheet resistance at 20 mM $AuCl_3$ concentration. This amount of change of R_s is comparable to the case of carbon nanotubes [30]. On the other hand, the doping stability was monitored over time, as shown in figure 2(b). After 20 days, R_s increased by less than 11% at the higher concentration of 10 mM $AuCl_3$, whereas it increased by up to 40% at a lower concentration of 1 mM $AuCl_3$. This indicates that the lower Au doping is less stable. This may be ascribed to the fact that the solvent nitromethane (CH_3NO_2) itself also dopes graphene to p-type [31]. However, in the case of CH_3NO_2, the molecule is volatile and will desorb after a certain time, which leads to an increased R_s as time goes on. For a lower $AuCl_3$ concentration, a higher percentage of the doping effect is induced by the CH_3NO_2 molecules, and thus the lower concentration ones are less stable. Another possibility is due to the hygroscopic nature of Cl^- ions; with moisture in the environment, the mobile Cl^- will combine with excess $AuCl_3$ to form $AuCl_4^-$ (see reaction (3)). Therefore,

with a higher concentration of $AuCl_3$, the excess $AuCl_3$ can continue to dope the graphene with moisture in ambient conditions via reaction (4). This might be another reason for the better stability of the doping effect with higher $AuCl_3$ concentration.

3.3. The charge transfer phenomena

To further elucidate the charge transfer between graphene and Au^{III}, the doped sample was characterized by Raman spectroscopy. The two prominent peaks in the Raman spectra of graphene are the G-band ($\sim$1584 cm^{-1}) involving phonons at the Γ point and the G′ band at $\sim$2700 cm^{-1} involving phonons near the K point (see the supplementary data, figure S4 available at stacks.iop.org/Nano/21/285205/mmedia) [32]. Evidence of the charge transfer has been detected from the G-band shift due to the phonon stiffening [33]. The G-band could be shifted by other effects such as temperature, surface charge, and strain [34–37]. However, in this work, these effects are excluded since the samples are measured under identical experimental conditions (temperature, laser power, etc) before and after the doping. The Raman spectra obtained from five different spots with a laser excitation energy of 532 nm (2.33 eV) were averaged with a standard deviation bar. A clear distinction in the doping effect between 1 and 2 layer graphene and multi-layer graphene layers was observed in figures 3(a)–(c). In the case of a multi-layer graphene layer (20–30 nm height confirmed by AFM), the G-band showed almost no shift with different $AuCl_3$ concentration. However, the G-band shift from 1 to 2 layer graphene initially rapidly increased and then saturated around 12 cm^{-1}, as shown in figure 3(d). The degree of charge transfer can be defined by the quantity f, which is the transferred charge per host C atom [38]. Using the $\Delta\omega/\Delta f \approx +460$ cm^{-1} for graphite intercalated compound (GIC), we estimated the degree of charge transfer between graphene and Au^{III}. We obtained $f \approx 1/38$, or one free hole per 38 C atoms, at 20 mM $AuCl_3$ concentration in 1–2 layer graphene regions only. Since Au particles were mostly formed on the small wrinkles with high curvature (less than 10 nm height) (figure 1(b)), the doping effect on the multi-layer graphene layer was weaker than that of 1–2 layer graphene.

3.4. Transparent conducting film

We further fabricated TCFs (0.25 cm^2) by transferring few layer graphene onto quartz and the poly(ethylene terephthalate) (PET) substrates. Figure 4(a) shows the transmittance of the film at 550 nm as a function of doping concentration. The transmittance of the film at 10 mM $AuCl_3$ concentration decreased by only about 2%, while the R_s was reduced by 77%. The transmittance was dramatically reduced by 4% at 20 mM $AuCl_3$ concentration due to the light absorption on the formed Au particles but the change of the sheet resistance was similar to that of the 10 mM $AuCl_3$ concentration. Therefore, the optimum doping concentration was chosen to be 10 mM. The opacity of the suspended graphene has been measured by Nair *et al* [2] and it was concluded that graphene's transmittance (T) and reflectance (R) are universal and given by $T \equiv (1 + 2\pi G/c)^{-2} = (1 + 1/2\pi\alpha)^{-2}$ and $R \equiv 1/4\pi^2\alpha^2 T$ for normal

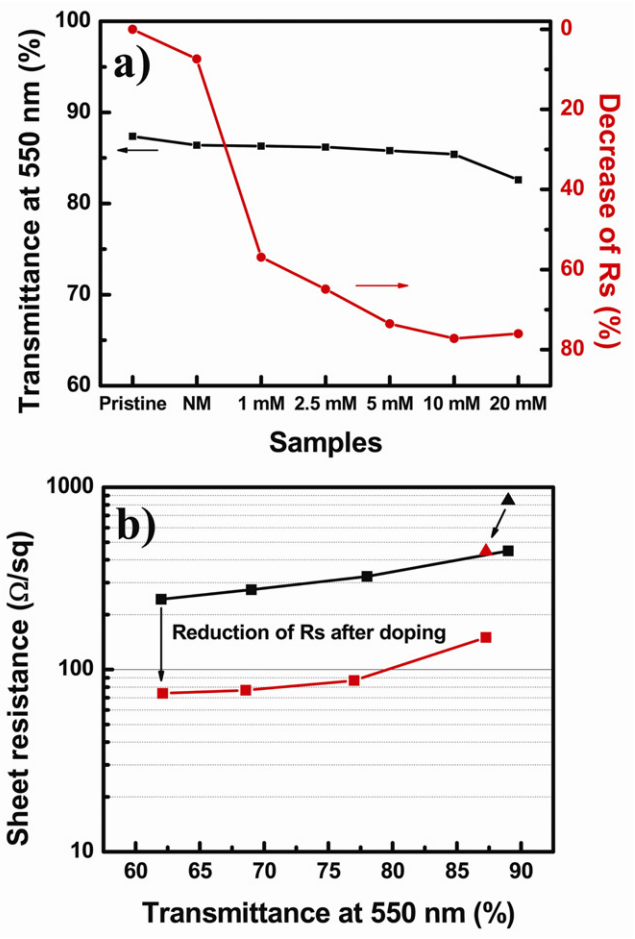

Figure 4. (a) Change of transmittance at 550 nm and R_s as a function of $AuCl_3$ concentration for graphene transferred onto the quartz substrate. (b) Transmittance versus R_s with an n-fold graphene film ($n = 1$, 2, 3, and 4) before and after $AuCl_3$ 10 mM doping. The triangle stands for graphene transferred onto PET film before and after doping, respectively.

light incidence, where G is the high frequency (dynamic) conductivity for Dirac fermions, $\alpha = e^2/\hbar c \approx 1/137$ is the fine structure constant, c is the speed of light, and h is Planck's constant. After calculating the absorption of light by two-dimensional Dirac fermions using Fermi's golden rule, this gives graphene's opacity $(1 - T) \approx \pi\alpha \approx (2.3\%)$. From the above relation ($T_{\text{layer}(n)} = (1-\pi\alpha)^n \times 100(\%)$), where n is the number of layers, we estimated the average number of layers of our graphene film to be five from the transmittance of 89% at 550 nm (see the supplementary data, figure S4 available at stacks.iop.org/Nano/21/285205/mmedia). A thicker graphene layer was prepared by multiple film transfer on top of each other, up to four times. The sheet resistance of the individual graphene film and the four fold graphene film were respectively 448 Ω/sq at $T = 89\%$ and 243 Ω/sq at $T = 62\%$ (at 550 nm), see figure 4(b). After doping with 10 mM $AuCl_3$, the R_s reached 150 Ω/sq at $T = 87\%$. For the purpose of a flexible TCF application our graphene film was transferred to PET. At this time, we could not anneal the film due to the low glass transition temperature of PET. The PMMA was removed only by acetone washing. The sheet resistance before and after

doping with 10 mM $AuCl_3$ concentration was 846 Ω/sq at $T = 89\%$ and 445 Ω/sq at $T = 87\%$ indicated by filled triangles, black and red color in figure 4(b), respectively. This relatively higher sheet resistance could originate from the breaking of the graphene sheet when PMMA was washed by acetone and a lower doping effect could come from the residual PMMA (see the supplementary data, figure S5 available at stacks.iop.org/Nano/21/285205/mmedia).

4. Conclusion

Graphene films transferred onto 300 nm SiO_2/Si, quartz, and PET were doped with $AuCl_3$ to increase their conductivity. The Au^{III} was reduced to Au particles by charge transfer from graphene to Au^{III}. Most of the Au particles were formed on the graphene wrinkles due to the de-localization of electrons by the curvature. The sheet resistance of the graphene film decreased by up to 77% depending on $AuCl_3$ concentration. The fabricated high-performance transparent conducting film with optimized doping concentration showed a sheet resistance of 150 Ω/sq at $T = 87\%$. Our graphene film, combined with the doping strategy, could be applicable to numerous areas such as solar cells, touch screens, and transparent displays in the future.

Acknowledgments

The authors gratefully acknowledge financial support for this work from Eni S.p.A. under the Eni-MIT Alliance Solar Frontiers Center. In addition, some of the authors received support from their home institutions. K K Kim acknowledges financial support from the National Research Foundation of Korea Grant funded by the Korean Government (NRF-2009-352-C00032) and Y H Lee acknowledges financial support from the MOEST through the TND project, STAR-faculty project, WCU (World Class University) program through the KOSEF funded by the MOST (R31-2008-000-10029-0), and the KOSEF through CNNC at SKKU. A Reina was supported by the Materials, Structure and Devices Center, one of the five centers of the Focus Center Research Program, a Semiconductor Research Corporation program. Y Shi and L J Li acknowledge the support of Nanyang Technological University.

References

[1] Novoselov K S, Geim A K, Morozov S V, Jiang D, Katsnelson M I, Grigorieva I V, Dubonos S V and Firsov A A 2005 *Nature* **438** 197
[2] Nair R R, Blake P, Grigorenko A N, Novoselove K S, Booth T J, Stauber T, Peres N M R and Geim A K 2008 *Science* **320** 1308
[3] Kim K S, Zhao Y, Jang H, Lee S Y, Kim J M, Kim K S, Ahn J-H, Kim P, Choi J-Y and Hong B H 2009 *Nature* **457** 706
[4] Li X, Zhang G, Bai X, Sun X, Wang X, Wang E and Dai H 2008 *Nat. Nanotechnol.* **3** 538
[5] Shin H-J *et al* 2009 *Adv. Funct. Mater.* **19** 1
[6] Eda G, Fanchini G and Chhowalla M 2008 *Nat. Nanotechnol.* **3** 270
[7] Geng H-Z, Kim K K, Kang K P, Lee Y S, Chang Y and Lee Y H 2007 *J. Am. Chem. Soc.* **129** 7758
[8] Kim H, Horwitz J S, Kushto G, Piqué A, Kafafi Z H, Gilmore C M and Chrisey D B 2000 *J. Appl. Phys.* **88** 6021
[9] Berger C *et al* 2006 *Science* **312** 1191
[10] Sutter P W, Flege J-I and Sutter E A 2008 *Nat. Mater.* **7** 406
[11] Reina A, Jia X, Ho J, Nezich D, Son H, Bulovic V, Dresselhaus M S and Kong J 2009 *Nano Lett.* **9** 30
[12] Li X *et al* 2009 *Science* **324** 1312
[13] Yu Q, Lian J, Siriponglert S, Li H, Chen Y P and Pei S-S 2008 *Appl. Phys. Lett.* **93** 113103
[14] Arco L G D, Zhang Y, Kumar A and Zhou C 2009 *IEEE Trans. Nanotechnol.* **8** 135
[15] Güneş F, Han G H, Kim K K, Kim E S, Chae S J, Park M H, Jeong H-K, Lim S C and Lee H Y 2009 *NANO* **4** 83
[16] Chae S J *et al* 2009 *Adv. Mater.* **21** 1
[17] Reina A, Son H, Jiao L, Fan B, Dresselhaus M S, Liu Z and Kong J 2008 *J. Phys. Chem.* C **112** 17741
[18] Reina A, Thiele S, Jia X, Bhaviripudi S, Dresselhaus M S, Schaefer J A and Kong J 2009 *Nano Res.* **2** 509
[19] Li X, Zhu Y, Cai W, Borysiak M, Han B, Chen D, Piner R D, Colobo L and Rouff R S 2009 *Nano Lett.* **9** 4359
[20] Abdou M S A and Holdcroft S 1993 *Synth. Met.* **60** 93
[21] Ciprelli J-L, Clarisse C and Delabouglise D 1995 *Synth. Met.* **74** 217
[22] Choi H C, Shim M, Bangsaruntip S and Dai H 2002 *J. Am. Chem. Soc.* **124** 9058
[23] Foley J D, van Dan A, Feiner S K and Hughes J F 1995 *Computer Graphics: Principles and Practice* (*Addison-Wesley Systems Programming Series*) (Upper Saddle River, NJ: Addison-Wesley)
[24] Blake P, Hill E W, Neto A H C, Novoselov K S, Jiang D, Yang R, Booth T J and Geim A K 2007 *Appl. Phys. Lett.* **91** 063124
[25] Roddaro S, Pingue P, Piazza V, Pellegrini V and Beltram F 2007 *Nano Lett.* **7** 2707
[26] Trasatti S 1986 *Pure Appl. Chem.* **58** 955
[27] Shan B and Cho K 2005 *Phys. Rev. Lett.* **94** 236602
[28] Novoselov K S, Jiang D, Schedin F, Booth T J, Khotkevich V V, Morozov S V and Geim A K 2005 *Proc. Natl Acad. Sci. USA* **102** 10451
[29] Seo K, Park K A, Kim C, Han S, Kim B and Lee Y H 2005 *J. Am. Chem. Soc.* **127** 15724
[30] Kim K K *et al* 2008 *J. Am. Chem. Soc.* **130** 12757
[31] Shin H-J, Kim S M, Yoon S-M, Benayad A, Kim K K, Kim S J, Park M H, Choi J-Y and Lee Y H 2008 *J. Am. Chem. Soc.* **130** 2062
[32] Ferrari A C *et al* 2006 *Phys. Rev. Lett.* **97** 187401
[33] Das A *et al* 2008 *Nat. Nanotechnol.* **3** 210
[34] Ni Z H, Yu T, Lu Y H, Wang Y Y, Feng Y P and Zhen Z X 2008 *ACS Nano* **3** 2301
[35] Calizo I, Bao W, Miao F, Lau C N and Baladin A A 2007 *Appl. Phys. Lett.* **91** 201904
[36] Ni Z H, Yu T, Luo Z Q, Wang Y Y, Liu L, Wong C P, Miao J, Huang W and Shen Z X 2009 *ACS Nano* **3** 569
[37] Calizo I, Balandin A A, Bao W, Miao F and Lau C N 2007 *Nano Lett.* **7** 2645
[38] Eklund P C, Arakawa E T, Zarestky J L, Kamitakahara W A and Mahan G D 1985 *Synth. Met.* **12** 97